

- **Attosecond physics:**  
*Metrology and applications of attosecond pulses .*

### 1. Introduction

Progress in optical pulse engineering over the last twenty years led to the generation of laser pulses with duration of few  $fs$  [1]. Such pulses have provided a unique tool for high resolution time domain spectroscopy, thus paving the way to the breakthrough of femtochemistry. However, a number of other processes in nature, mainly related to the ultrafast dynamics of electronic motion, evolve with characteristic times of the order of one femtosecond or even shorter. *Sub-fs* resolution is the central requirement for time domain studies of such processes. The generation, characterization and proof of principle applications of pulses depicting attosecond ( $as$ ) localization is the target of the since recently debuting *attosecience*.

The principle of the generation of  $as$  pulse trains is similar to that of mode locked  $fs$  lasers. Temporal energy localization comes about in wave mechanics whenever mutually coherent waves are superimposed in time and space. In a the simplest idealized case, when monochromatic waves of equally spaced and properly phased frequencies are superimposed, the total field depicts a temporal beating with a repetition rate equal to half of the frequency spacing. A train of pulses is formed. For perfect phase locking, i.e. when there is no phase difference between the different spectral components, the degree of localization is inversely proportional to the number of the phase locked frequency components. The resulting train pulses are known as Fourier transform limited (FTL), as there duration is the smallest allowed and equal to the time domain spectrum width that is obtained from a Fourier transformation of the frequency domain spectrum. For the generation of an  $as$  pulse train the comb of equally spaced frequencies has to be in the UV/VUV-XUV or x-ray spectral regions. The non-linear process known as higher order harmonic generation, occurring when an intense laser field interacts with an atomic gas, offers best prospects for the generation of  $as$  pulses [2,3]. In this sense, the harmonic emission from atoms is considered as the most suitable process for the achievement of temporal localization of light to these unprecedented short time scales.

The generation of harmonics of an IR  $fs$  laser with XUV photon-energies higher than ionization-threshold of the generating atom the emission is successfully described by a quasi classical three-step model offering intuitive pictures of the generation dynamics and allowing coupling of the atomic emission with propagation in the generating medium [4-7] (Fig. 1a).

In this model the combined oscillating potential of the atom and laser electric field forms a local time dependent barrier through which a bound electron can tunnel or escape over it at a given phase of the driving field (1<sup>st</sup> step). Subsequently, the almost free electron moves classically in the continuum gaining energy from the driving field and eventually revisits the parent ion with a given kinetic energy that depends on the moment of its birth and its trajectory in the continuum (2<sup>nd</sup> step). Upon return to the vicinity of the parent ion (third body) the electron may recombine to

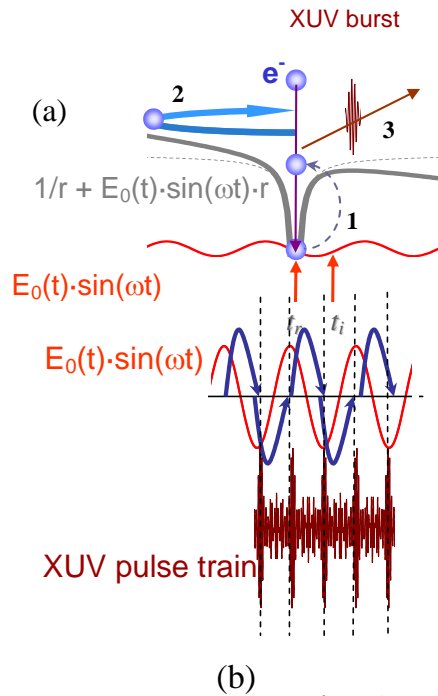


Fig. 1

emit a burst of energetic radiation (3<sup>rd</sup> step). Coherent periodic repetition of these dynamics twice per optical cycle, leads to a discrete emission spectrum of the odd harmonics (in accordance with angular momentum and parity conservation) of the driving laser field (Fig. 1b).

The energy that the electron gains in its trajectory in the continuum and the time of recombination depend sensitively on the phase of the driving field at the moment the electron is ejected. Those are the parameters that will finally define the temporal width of the emitted radiation bursts.

From a rigorous treatment it turns out that essentially two trajectories contribute to the generation of a harmonic. These two are known as the “long” and “short” trajectories due to the different duration of the electron excursion in the continuum.

Furthermore proper propagation conditions are shown to eliminate the long trajectory [8]. The surviving short trajectory determines the *as* generation dynamics.

## 2. Metrology

The first indication of laboratory *as* pulse trains came in 1999 [9]. The proper characterization of XUV *as* pulses became a challenging problem. Well-established *fs* metrology relies on a non-linear effect induced solely by the radiation to be characterized. Already a 2<sup>nd</sup> order (AC) allows the determination of the pulse duration to a satisfactory degree of accuracy. That is why it has been routinely used for many years in *pico*- and *fs* laser laboratories. Its extension to *sub-fs* XUV pulses is far from trivial as they are orders of magnitude weaker than the laser radiation, spectrally much broader and in the notoriously most difficult spectral region to handle. No beam splitters are available for the autocorrelator and the fragility of the pulses requires highly dispersionless optical arrangements. The non-linear detector has to rely on a two-photon process, such as two-photon ionization. Its cross-section requires high intensities and a detector with a flat response over the broad frequency spectrum. Those are the obstacles that prevented for several years a successful measurement of a 2<sup>nd</sup> order AC of *as* pulses and have forced the diagnostics to cross-correlation based approaches between the IR laser field and that of the XUV radiation.

The approaches of the collaboration of FORTH-IESL with MPQ Graching towards the solution of the above problems and the final successful implementation of the 2<sup>nd</sup> order autocorrelation measurement of an *as* pulse train [10,11] are as follows:

### 2.1 Development of dispersionless broadband XUV autocorrelator

In the quest of a solution to the problem of the dispersionless broadband XUV autocorrelator two different set-ups have been designed, developed and tested.

#### The transmission grating Michelson interferometer

Although the first one could not be used in the 2<sup>nd</sup> order AC measurement of higher harmonics at their present intensity level, its excellent properties offer a valuable tool to the metrology and applications of the XUV radiation of brighter sources and thus it is worth outlining its operation here.

It is a Michelson type interferometer [12] arrangement in which the beam splitter/combiner is a free standing transmission grating (Fig. 2). Zero and

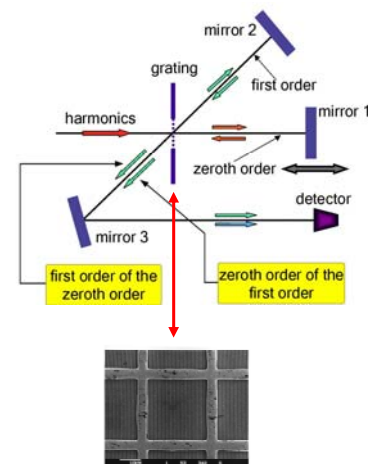


Fig. 2

first order diffraction rays of the same frequency are retro-reflected and recombined at the grating through first and zero order diffraction respectively. Correlation measurements can be performed by translating one of the two spherical mirrors (M1 or M2). For the ideal case of a single ray it becomes immediately apparent that equal optical paths guarantee dispersionless operation. For the realistic case of extended and diverging beams ray tracing analysis [38] has shown that by imaging the grating on the detector, the set up is dispersionless down to the 1as regime.

The interferometer has been tested in the *fs* regime in measuring a 2<sup>nd</sup> order autocorrelation of the third harmonic (fig. 3) [13] of the Ti:Saph laser system of FORTH-IESL (800nm, 2mJ, 50fs, 1KHz rep. rate).

The set up has a flat spectral response for a very large energy range, with lower and upper limits set by the grating constant and the absorption edge of the grating material. At the same time it allows for wavelength selection using slits or knife edges in the parts where the radiation is spatially dispersed. A serious drawback is its lower than 1% throughput, due to the double diffraction. Thus this arrangement is only appropriate for cross-correlation measurements of higher harmonics with the IR fundamental frequency or for non-linear AC measurements of intense XUV radiation like that foreseen for the advanced XUV/x-ray sources based XFELs.

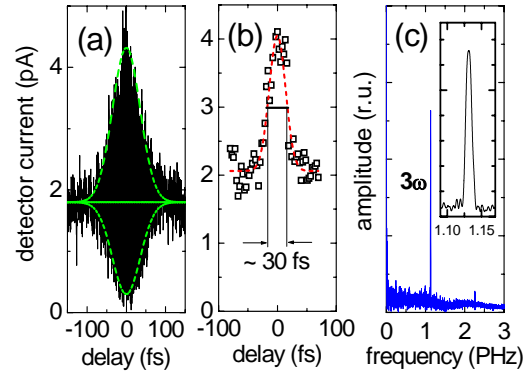


Fig. 3

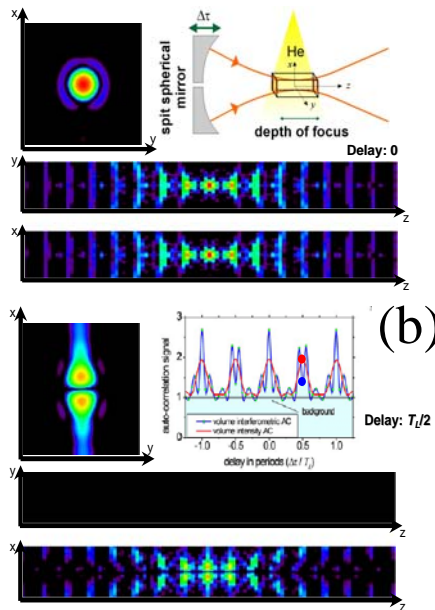
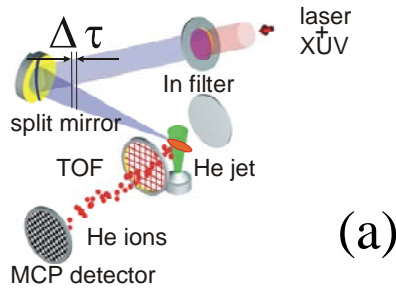


Fig. 4

#### The split spherical mirror autocorrelator

A more efficient autocorrelator design is that of the slit spherical mirror (Fig. 4(a)) [10,11].

This arrangement can be used for a 2<sup>nd</sup> order AC measurement by piezoelectrically translating one of the two mirror halves. Unlike the amplitude splitting arrangements (conventional Michelson), this technique is a wavefront splitting device. As such, a delay variation results not in a change of the total energy reaching the detector, but simply in a spatial redistribution of the energy in the focal volume. The 3D intensity distribution at the focal area for the superposition of the 7<sup>th</sup> to the 15<sup>th</sup> harmonic is shown for a delay of 0 and  $T_L/2$  in Fig. 4b. *z* is the propagation axis and the cut of the mirror is parallel to the *y* axis. This local intensity rearrangement induces a modulation in the measured signal as shown with the blue curve in the insert of the lower Fig 4b panel (interferometric autocorrelation trace). The peak to background ratio in an intensity autocorrelation trace (red curve in the insert of the lower Fig 4b

panel) measured with this device is reduced to 2 as compared to the ratio of 3 of a conventional AC, but is still high enough to observe a modulated signal from which the mean value of the *as* individual train pulses (“wagons”) is extracted.

### 2.2 The broadband non linear XUV detector

The superposition of the harmonics that has been characterized through a 2<sup>nd</sup> order autocorrelation measurement includes the 7<sup>th</sup> to the 15<sup>th</sup> harmonic of the Ti:Sapph laser emitting at 790nm. The relative intensity amplitudes of the harmonics reaching the He jet are 7:9:11:13:15 → 0.32:1.0:0.30:0.11:0.01. For this harmonics the non-linear broadband XUV detector chosen is based on the two-photon ionization of He induced by the radiation to be characterized [14,15], i.e. the generated and transmitted by an In filter harmonic superposition (Fig. 4a). The relevant ionization channels are shown in Fig. 5. He ions are then detected through a time of flight mass spectrometer.

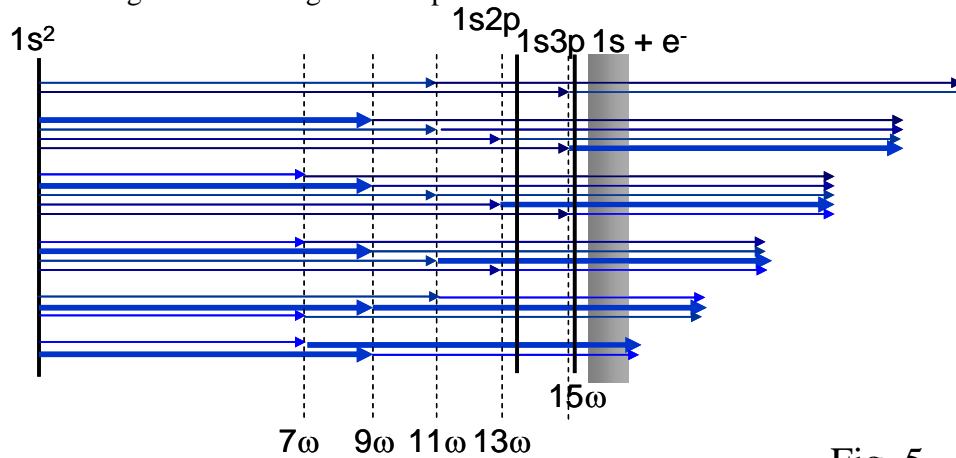


Fig. 5

The experimental evidence of observed two-XUV-photon ionization is given by the measurement of the three different ion ( $\text{He}^+$ ,  $\text{H}_2\text{O}^+$  and  $\text{Xe}^+$ ) yields in the time of flight mass

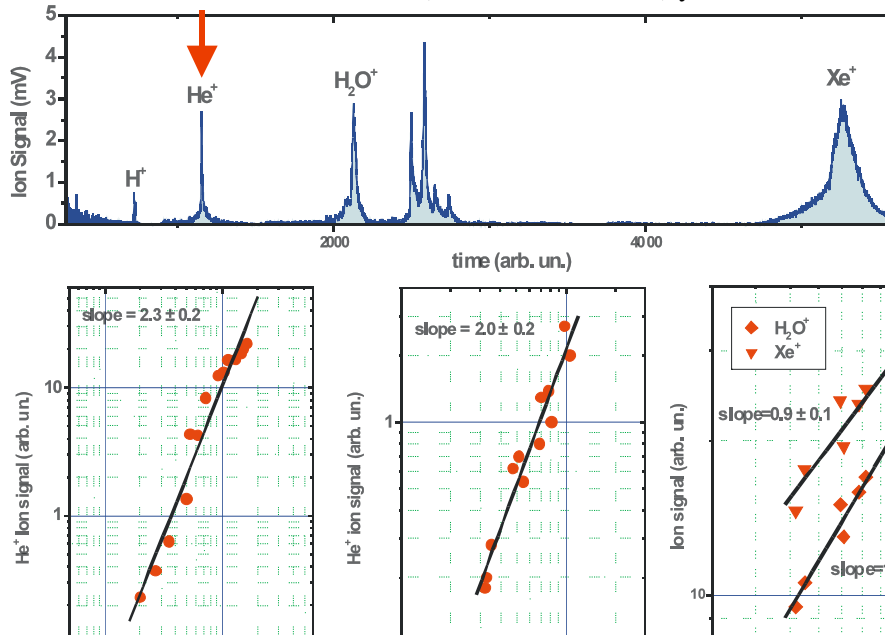


Fig. 6

spectrum (Fig.6 upper panel) as a function of the XUV intensity. H<sub>2</sub>O and Xe have low ionization potentials (IPs), 12.6 eV and 12.1 eV respectively, as compared to the 24.6 eV IP of He and thus for the given XUV wavelengths ionize predominantly through single photon absorption. In log-log scale the intensity dependence for He<sup>+</sup> is very nearly quadratic while for H<sub>2</sub>O<sup>+</sup> and Xe<sup>+</sup> is linear (Fig. 6 lower panels). Based on LOPT, the measured slopes provide clear evidence of a two-photon ionization of He.

This two-XUV-photon detector further fulfils all requirements relevant to a 2<sup>nd</sup> order AC measurement. Its spectral and temporal response has been theoretically investigated. The energy resolved yields for the same harmonic superposition have been *ab initio* calculated by numerically solving the 3D TDSE of He in the polychromatic field of the harmonic superposition. For the spectral region of interest, the deviation from an entirely flat response is of the order of 30%. This deviation does not affect the measured duration, as verified by further quantum calculations of 2<sup>nd</sup> order autocorrelation traces. The autocorrelation trace of the quantum calculation is identical to the autocorrelation trace of a detector having instantaneous temporal response. These calculations further provide clear evidence that the time response of the detector is also not distorting the measured durations, at least at the temporal level of 100as. An instantaneous temporal response is not *a priori* valid for the two photon process at this temporal scale. This rigorous assessment of the detector indicates optimal operational specifications [16].

## 2.2 The 2<sup>nd</sup> order autocorrelation of an XUV pulse train.

Applying this technique to the superposition of the 7<sup>th</sup>-15<sup>th</sup> harmonics the autocorrelation trace of Fig. 7a has been recorded. This is the first direct experimental observation of an *as* pulse train [10,11]. From the fitting of a series of Gaussian distributions a mean pulse duration of  $(780 \pm 80)$  *as* has been extracted. Using the same technique at lower temporal resolution and a larger delay interval the duration of the train envelope has been determined Fig. 7b. The total number of photons in the train is  $\sim 10^{10}$ - $10^{11}$  and in each burst  $\sim 10^9$ - $10^{10}$ . The focused intensities reached are of the order of  $10^{11}$ W/cm<sup>2</sup>. The measured duration of the individual pulses is more than twice its Fourier transform limited (FTL) value of  $\tau_{XUV} = 315$  *as*. An estimation of this duration, from the phases resulting by the short trajectory including the additional spatiotemporal chirp of each harmonic originating from the spatiotemporal laser intensity distribution at the generation volume is in reasonable agreement with the measurement [16].

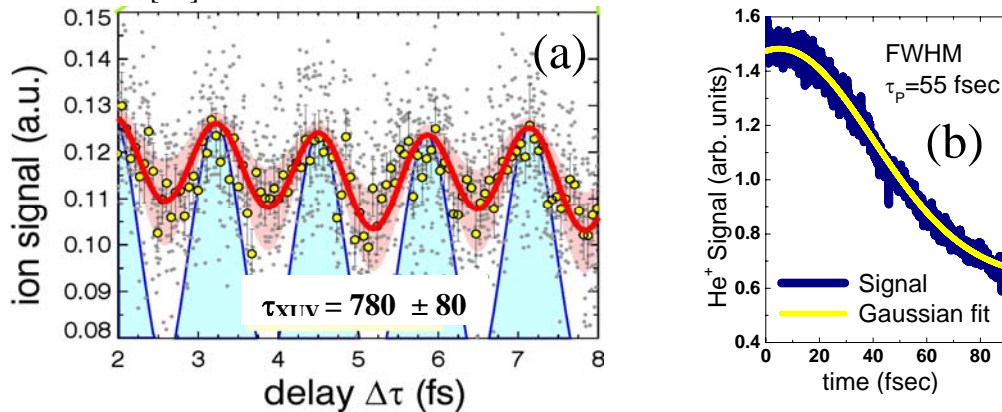


Fig. 7

The 2nd order autocorrelation measurement, once established as an attosecond metrology tool, can be extended, by employing energy resolved photoelectron spectroscopy instead of mass spectroscopy, to a second order frequency resolved XUV Gating, a FROG [17] type of measurement in the XUV spectral range. This is currently in progress at IESL and is expected to allow almost full retrieval of the pulse shapes and the measurement of the variation of the pulse duration of the individual wagons within the train envelope.

The described 2nd order AC experiment opens further up the field of applications of attosecond pulses by means of XUV-pump XUV-probe studies of ultra-fast dynamics. The present experiment is in fact an example of such an application. The attosecond pulse train pumps an electronic wave packet in the virtual state of the two-photon ionization process. The temporal evolution of this wave packet is probed through the ionization step of the two-photon process. Since the evolution of the wave packet (as shown by our calculation) follows the E -field of the harmonic superposition it reveals its temporal characteristics. Furthermore the approach offers metrology and application solutions for future research to be conducted with XFEL based light sources. Due to the high repetition rate and delivered photon fluxes of such sources our developments are expected to be particularly useful.

1. G. Steinmeyer et al. *Science* 286 (1999) 1507.
2. T. W. Hänsch *Opt. Comm.* 80 (1990) 71.
3. Gy. Farkas et al. *Phys. Lett. A* 168 (1992) 447.
4. P. B. Corkum: *Phys. Rev. Lett.* 71 (1993) 1995.
5. M Lewenstein et al. *Phys. Rev. A* 49 (1994) 2117.
6. W. Becker et al. *Adv.At. Mol. Opt. Phys.*,48 (2001) 36.
7. F. Lindner et al. *Phys. Rev. A* 68 (2003) 013814.
8. M. B. Gaarde et al. *Phys. Rev. Lett.* 89 (2002) 213901.
9. N. A. Papadogiannis et al. *Phys. Rev. Lett.* 83 (1999) 4289.
10. P. Tzallas et al. *Nature* 426 (2003) 267.
11. P. Tzallas et al. *J. Mod. Opt.*
12. E. Goulielmakis et al. *Appl. Phys. B* 74 (2002) 197
13. N.A. Papadogiannis et al. *Opt. Lett.* 27 (2002) 1561.
14. N.A. Papadogiannis et al. *Phys. Rev. Lett.* 90 (2003) 133902;
15. N. A. Papadogiannis et al. *Appl. Phys. B* 76 (2003) 721.
16. L.L.A. Nikolopoulos et al. (submitted)
17. R. Trebino et al. *JOSA A* 10 (1993) 1101.